

# Nanoscale Control of the Surface Functionality of Polymeric 2D Materials

Oksana Suraeva, Anke Kaltbeitzel, Katharina Landfester, Frederik R. Wurm, and Ingo Lieberwirth\*

Typically, 2D nanosheets have a homogeneous surface, making them a major challenge to structure. This study proposes a novel concept of 2D organic nanosheets with a heterogeneously functionalized surface. This work achieves this by consecutively crystallizing two precisely synthesized polymers with different functional groups in the polymer backbone in a two-step process. First, the core platelet is formed and then the second polymer is crystallized around it. As a result, the central area of the platelets has a different surface functionality than the periphery. This concept offers two advantages: the resulting polymeric 2D platelets are stable in dispersion, which simplifies further processing and makes both crystal surfaces accessible for subsequent functionalization. Additionally, a wide variety of polymers can be used, making the process and the choice of surface functionalization very flexible.

a hydrophilic surface.<sup>[10]</sup> In addition to the different chemical functionalization of the two basal surfaces, sequential methods can also be used to achieve a locally structured surface. Merg et al. were able to demonstrate nanosheets with a core-shell structure based on collagen-mimicking peptides.<sup>[11]</sup> For this they used the method of temperature controlled seeded growth.

However, the control over the lateral structure in 2D materials is still a challenge. We therefore present here a new and simple concept based on the crystallization of polymers which also exploits the principles of temperature controlled seeded growth. The starting point is two precisely synthesized polymers with different functional groups integrated into

the main chain. When these two different polymers are crystallized sequentially from a solution, nano-platelets with different surface functionalization in the center and at the periphery are obtained.

Recent works<sup>[12–16]</sup> show that polymer crystallization is a promising approach to produce well-defined 2D nanosheets. To gain control over the local arrangement of chemical functionalities during the self-organization of molecules or polymers, the group of Manners has developed basic concepts.<sup>[17,18]</sup> They synthesized ferrocene-based block copolymers containing a crystallizable polyferrocenyldimethylsilane (PFS) block and a non-crystallizable block, which can be easily functionalized. By covalently attaching different fluorophores to the block copolymer and subsequent crystallization-driven self-assembly (CDSA) of the polymers, they were able to form 1D micelles with segmentally controlled chemical functionalization. However, labeling with the respective dyes was carried out exclusively prior to the structure-forming crystallization and the associated formation of micelles.


Herein, we take a step further and first perform the structure formation of the nano-platelets. Only afterward do we exploit the different chemical identity of the surface functionalization using a selective chemical reaction. We use – in contrast to the block-co-polymers used in previous works – precisely synthesized homopolymers. This polymer consists of a polyethylene (PE) chain with equidistantly incorporated functional monomer units. If we now perform a solution crystallization with two differently functionalized polymers, we obtain a nano-platelet that has different chemical functionalization in the center than at the periphery. In this process, it is important that the two

## 1. Introduction

2D organic materials are of interest for membrane applications, in biomedical settings,<sup>[1]</sup> as high surface area adsorbents, catalyst supports and sensors.<sup>[2,3]</sup> Various conceptual approaches for the production of 2D organic layer systems have already been discussed extensively in the current literature.<sup>[4,5]</sup>

For example, Yang et al. used conjugated polymers to generate uniform, semiconducting nanosheets.<sup>[6]</sup> These structures grow uniaxially and due to the lack of defects or chain folding, the kinetics of the polymer self-assembly is similar to living polymerization. Another promising approach is the use of sequence defined, peptoid-based molecules.<sup>[7–9]</sup> Due to their biocompatibility, these structures are well suited for biomedical applications. Moreover, peptoid-based systems also allow a well-controlled, local structuring. For example, Lin et al. demonstrate the formation of Janus like nanosheets with a hydrophobic and

O. Suraeva, A. Kaltbeitzel, K. Landfester, F. R. Wurm, I. Lieberwirth  
Department of Physical Chemistry of Polymers  
Max Planck Institute for Polymer Research  
Ackermannweg 10 55128, Mainz, Germany  
E-mail: lieberw@mpip-mainz.mpg.de

 The ORCID identification number(s) for the author(s) of this article can be found under <https://doi.org/10.1002/sml.202206454>.

© 2023 The Authors. Small published by Wiley-VCH GmbH. This is an open access article under the terms of the Creative Commons Attribution License, which permits use, distribution and reproduction in any medium, provided the original work is properly cited.

DOI: 10.1002/sml.202206454

polymers crystallize one after the other. The heterogeneous functionalization on the surface of the nano-platelets can be used for regioselective chemical reactions. In this report, we functionalized the OH groups in the periphery of the nano-platelets locally by the reaction with trimethylchlorosilane. This is the first proof that it is possible to achieve a laterally structured chemical functionalization on the surface of polymer nanosheets through sequential polymer solution crystallization (SPSC).

## 2. Results and Discussion

To generate laterally structured nanosheets, we exploit the solution crystallization of polyethylene (PE), a very common and well-known polymer. It has been known since the works of Keller<sup>[19]</sup> and Fischer<sup>[20]</sup> in 1957 that semi-crystalline polymers like PE, crystallize in a lamellar morphology. Here, the polymer chain passes through the crystal lamella perpendicular to the basal surface of the crystal. At the two basal surfaces, the chain folds back and re-enters the crystal. In this way, a surface with regular chain backfolds is formed. The crystallization of polymers proceeds via the formation of stable nuclei, which then continue to grow. The thickness of the crystal lamella is determined by the supercooling according to the Gibbs–Thomson equation. The crystals thus formed have a thickness that is disparagingly small compared to the lateral size. Thus, the solution-crystallized polymer crystals can be regarded as 2D organic layers or nanosheets. Furthermore, during crystallization, any molecular defects in the polymer chain, such as branching, are expelled out from the crystal to the surface due to steric hindrance. A polymer chain with equidistantly distributed defects will, in contrast to classical nucleation, form lamellae which a thickness corresponding to the defect spacing in the chain.<sup>[21]</sup>

For our concept, we use precisely architected PE. Using acyclic diene metathesis (ADMET),<sup>[22]</sup> we synthesized a PE with integrated vitamin C functional groups equidistantly distributed along the main chain. Because of the steric hindrance, these functional groups are expelled from the crystal to the basal surface of the crystalline nanosheets during the crystallization of the polymer, and are thus supposed to arrange in a precise periodic crystal pattern on the surface.<sup>[23]</sup> The thickness of the nano-platelets can be easily adjusted via the distance between the functional groups in the chain.<sup>[21]</sup> Based on this, we can now apply sequential crystallization of the differently functionalized PE one after the other so that we obtain the desired surface-structured nano-platelets.

First, we demonstrate the 2D organization of a polyethylene with equidistant vitamin C functional groups,<sup>[24,25]</sup> which were labeled with two different dyes prior to crystallization. Using SPSC, we can generate nanosheets that are marked with a different dye on the outside and inside of the sheet. To demonstrate the versatility of this SPSC-based method for precision polymers, we co-crystallize two differently functionalized precision polymers that have the same length of alkyl units between the functional groups. Here, a polyphosphoester and a vitamin C-polymer, each with 20 CH<sub>2</sub> units between the functional groups, were crystallized from a common solvent. Due to the different crystallization kinetics of the polymers used, locally

structured nanosheets were formed in which the polyphosphoester is first crystallized as a seed and then the vitamin C-PE grew in a frame around the crystal presented. To prove the locally structured chemical functionalization of the nanosheets thus formed, the OH groups of the vitamin C were functionalized by means of trimethylsilyl chloride (TMSCl), forming silyl ether. The principal approach of using different functionalized precision polymers to form laterally structured 2D organic nanolayers is shown in **Scheme 1**.

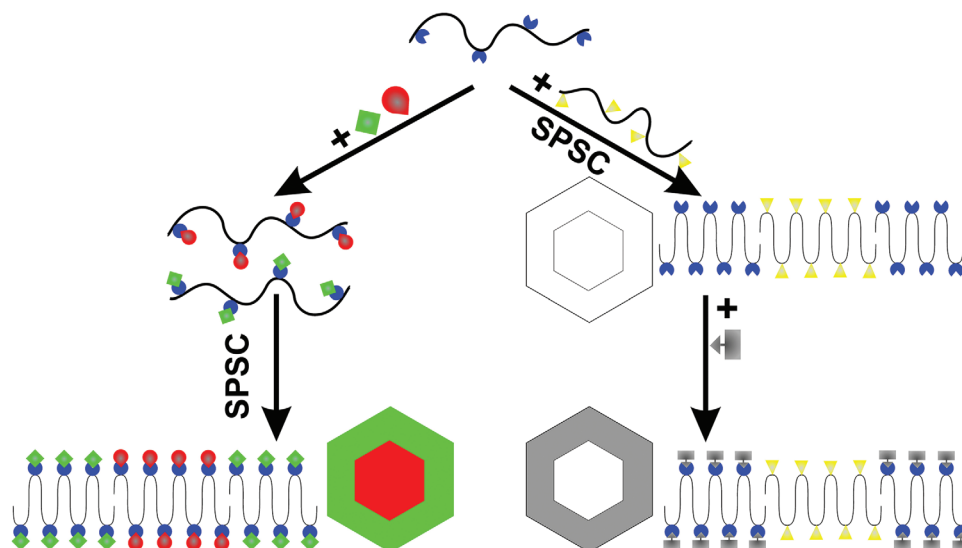
Starting point for the investigation into successive crystallization is a polyethylene with vitamin C groups at an exact distance of 20 CH<sub>2</sub> units. These vitamin C units act as defect during the crystallization process, causing the polymer chain to re-fold and push the vitamin C units to the surface of the crystal. This results in the formation of a lamellar crystal with a thickness of 20 CH<sub>2</sub>, which is ≈3 nm.<sup>[24]</sup> Additionally, since the arrangement of the vitamin C units is based on the crystallization process of the polyethylene, they are arranged on the crystal surface with the same perfection as the crystal lattice.

To determine whether covalently binding different molecules, in this case the dyes Cy3 and Cy5, would affect the crystallization of the two batches, we covalently attached the two dyes to the vitamin C PE (Scheme S1, Supporting Information). For polymers, it is known that even small differences in the molecular structure can lead to segregation.<sup>[26,27]</sup> This would also rule out a successive crystallization or co-crystallization of the two differently modified polymers.

The covalent attachment of the dyes to the polymer was confirmed using HPLC (Figure S1, Supporting Information). To investigate the impact of this chemical modification on co-crystallization of the two dye-labeled polymers, we performed crystallization experiments on a water surface in a Langmuir–Blodgett trough (LBT). We prepared a low concentration THF solution of each of the two differently labeled polymers, and dropped a few drops of these solutions onto the water surface to form a thin film of the polymer solution. After evaporation of the solvent, the nanosheets remain in the form of lamellar polymer crystals. If the two differently labeled polymer solutions were mixed beforehand, co-crystals are formed from the two labeled polymers, as can be seen from the orange crystals in **Figure 1a**. If the polymer solutions were applied one after the other, two independently fluorescent green and red crystals were detected (**Figure 1b**).

The conclusion from these observations is that the two differently marked polymers can crystallize jointly (**Figure 1a**). A sequential crystallization by adding Cy5 labeled polymer to existing crystals of Cy3 labeled polymer (or vice versa) was not possible in this experimental configuration. We only obtained completely green and red, but no locally structured nanosheets. We suspect that the fast evaporation of THF is the main cause. Accordingly, the crystallization is too fast, so that a homogeneous crystallization starts immediately and thus the presented crystals do not grow further by adding the second polymer from solution. It is therefore a question of controlling the polymer crystallization to achieve sequential growth of the crystals.

To optimize the crystallization process and to get access to each crystal, all following experiments were not conducted on a water surface but in solution instead. As solvents, we used ethyl acetate and a THF–water mixture. Upon crystallization,



**Scheme 1.** Two ways to form polymer 2D materials with spatial control over the surface functionality at the nanoscale: the functional groups of the polymer are modified prior (left) or after (right) the structure forming sequential polymer solution crystallization. The functional groups are expelled to the surface of the nanosheets yielding a template of functional groups with the perfect lattice arrangement from the polymer crystal. Left: a vitamin C-PE is labeled with two different dyes and subsequently crystallized using SPSC yielding polymer nanosheets with, for example, a red core and a green periphery. Right: Two differently functionalized PE, vitamin C and polyphosphoester, are co-crystallized resulting in nanosheets with a core made of PPE and a rim made of vitamin C-PE. Subsequently, the OH groups of the vitamin C-PE were used to locally precipitate silyl ether.

the vitamin C-PE forms monolayer 2D crystals in solution. Concentration and temperature are the crystallization controlling factors.<sup>[28]</sup> In THF–water mixtures the ratio between the two solvents plays an additional and important role.<sup>[29,30]</sup>

The crystallization process from THF–water mixtures yields monolayer crystals as well. With the addition of water to the THF–polymer solution, the polymers' solubility decreases and thus induces the crystallization. The resulting dispersion of the 2D nanosheets was stable for several weeks due to the amphiphilic nature of the polymer. To find optimal crystallization parameters, a series of experiments with different polymer concentrations was carried out with a solvent ratio THF:water = 4:1. A concentration in the range of 0.1–0.25 mg mL<sup>-1</sup> was found

optimal to create monolayer crystals, which did not agglomerate according to the TEM observations (Figure S2, Supporting Information).

We were able to regulate the size of the crystals easily by adjusting the THF:water ratio (Figure S3, Supporting Information). Since water is a poor solvent for the polymer, it induces the formation of crystal nuclei. Increasing the amount of water increases the nucleation density and thus the amount of initial crystallization seeds. As a result, more polymer crystals are generated. Accordingly, the crystals are smaller. In contrast, conducting the experiment with a lower amount of water in the mixture helps to increase the lateral size of the crystals (Figure 2A). Hence, we can easily control

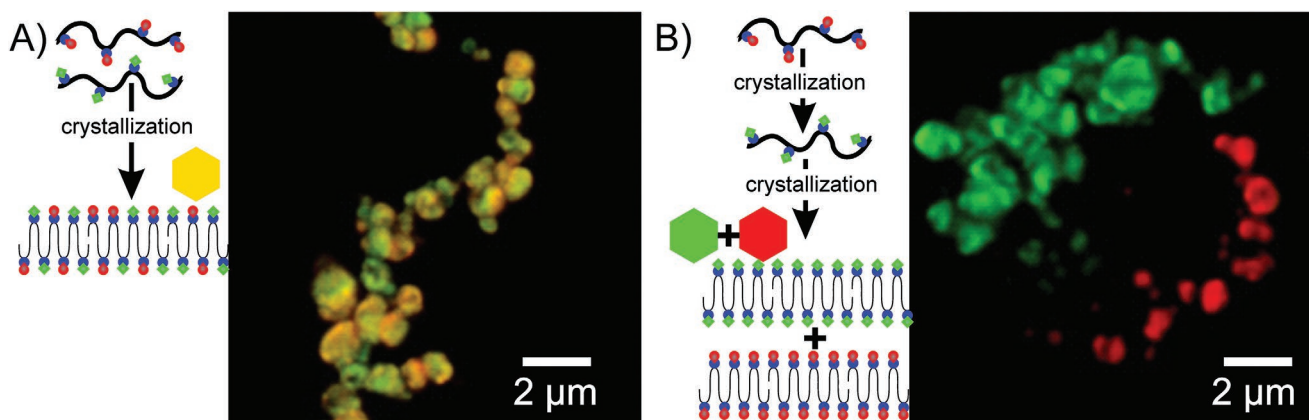


**Figure 1.** cLSM micrographs of fluorescent labeled vitamin C-PE nanosheets. The diluted THF solutions have been mixed before we applied them to a water surface of a LBT (A). The two polymers co-crystallize forming a random mixture of red and green dye polymer in every polymer nanosheet. When we apply the two diluted solutions of red and green labeled polymer subsequently (B), the resulting polymer nanosheets are uniformly labeled with red or green dye, only.

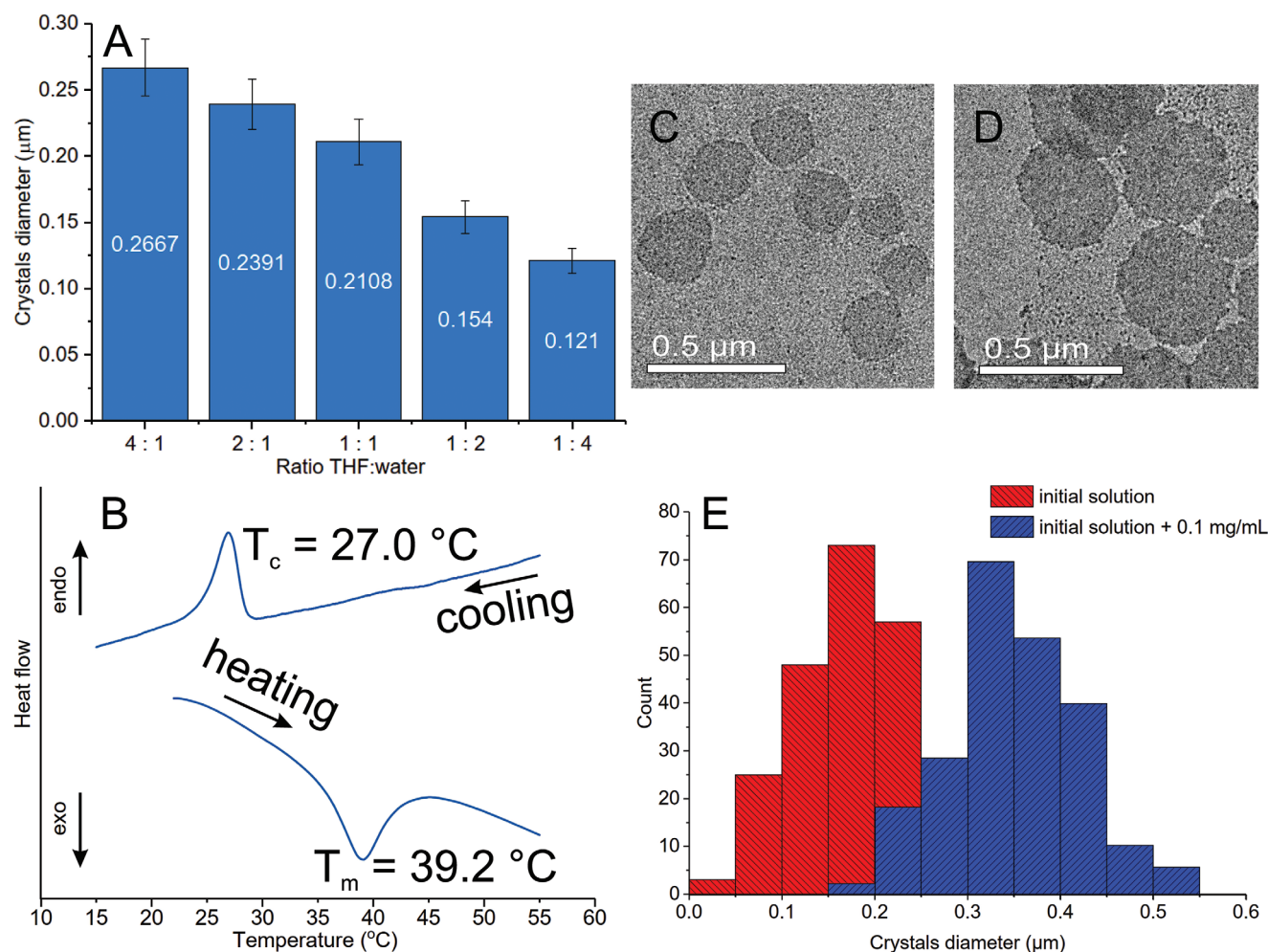


**Figure 2.** Dependence of polymer crystal size on the THF:water ratio (A), DSC thermogram of polymer crystals in dispersion in a 3:2 THF:water mixture (B), TEM bright-field micrograph of solution grown single crystal of initial solution  $0,08 \text{ mg mL}^{-1}$  (C) and initial solution +  $0.1 \text{ mg mL}^{-1}$   $38 \text{ }^\circ\text{C}$  (D) from a THF:water mixture and the corresponding crystal size distribution (E).

the lateral size of the 2D nanosheets by the water content of the THF–water solution.

In the next step, we want to continue the crystal growth process by adding additional polymer solution to the already formed dispersion of polymer crystals in the THF:water mixture (Figure S4, Supporting Information). As expected, the lateral size of the crystals increased from 173 nm for the initial dispersion to 217 and 263 nm after addition of 0.05 and 0.15 mg of the vitamin C-PE, respectively. However, besides the larger crystals, a substantial amount of small crystals also formed during this process. As this two-step crystallization was conducted at room temperature, it is very likely that the small crystals formed immediately due to the poor solubility in the THF–water system. The existing crystals grew with the addition of the second polymer portion.

By adjusting the temperature, separate nucleation after the addition of the second fraction of the polymer was suppressed and forced it to crystallize on the existing seeds instead. To optimize this process and to find the optimal temperature, DSC measurements of the polymer crystals in dispersion were conducted (Figure 2B). In contrast to melting and crystallization in

bulk,<sup>[11]</sup> for the dispersion of monolayer crystals these processes occurred at much lower temperatures. The vitamin C-PE crystals melt (or dissolve) at  $39 \text{ }^\circ\text{C}$  and crystallize at  $30 \text{ }^\circ\text{C}$ . This defines the temperature window in which existing crystals are stable and dissolved polymer does not crystallize.

Thus, carrying out the crystal growth experiment at  $38 \text{ }^\circ\text{C}$  revealed a completely different picture (Figure 2D and Figure S5, Supporting Information). Initial crystals, prepared at room temperature, have an average size of 208 nm (Figure 2C). Next, this dispersion was heated to  $38 \text{ }^\circ\text{C}$ , taking care not to exceed this temperature. Subsequent addition of 0.1 mg of vitamin C-PE at  $38 \text{ }^\circ\text{C}$  followed by a very slow cooling to room temperature yields crystals with av. size of 367 nm. No small crystals were observed this time. Accordingly, the size distribution of the lateral crystal size shifts to larger values (Figure 2E). Moreover, it should be emphasized that even the variance (or polydispersity) of the size distribution is not significantly altered after the secondary growth process; the size distribution remains relatively narrow. This indicates that the added portion of polymer solely crystallizes on the exterior of the provided initial crystals. However, in the TEM micrographs (Figure 2D) this core-rim

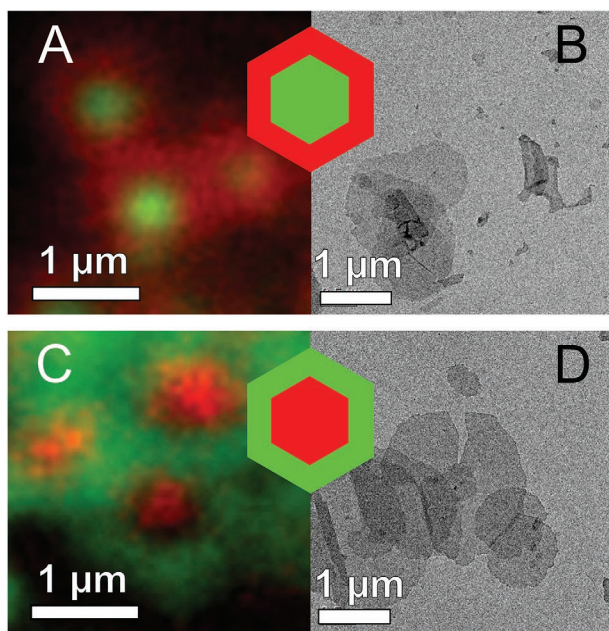


**Figure 3.** Schematic illustration of the crystals with core–shell structure, TEM bright-field micrographs (B and D) of solution grown crystals and confocal microscope imagerimages (A and C), revealing the desired structure. Red color—vitamin C-PE labeled with Cy5 dye, green color—vitamin C-PE labeled with Cy3 dye.

structure is invisible, because the same polymer was used for initial and secondary crystallization.

With this optimized process at hand we now come back to the fluorescent labeled vitamin C polymers to demonstrate the potential of the sequential CDSA process: crystals with a red-labeled core and a green-labeled shell (or vice versa). The nanostructured lamellar single crystals shown in **Figure 3** have been prepared using the above process, starting with, for example, the red-labeled polymer as initial crystals. In the second step, the green-labeled polymer was added, forming the outer rim of the nanosheets. From the TEM micrographs, there is again no difference visible between the core and the shell polymer of the nanostructured 2D nanosheet crystals. However, confocal scanning laser microscopy clearly demonstrates the successful SPSC process. Since the polymers used for the core and for the shell are identical except for the fluorescent labeling, the order can be reverted at will to start with either a red or a green core, as demonstrated in **Figure 3**. Therefore, our concept of SPSC indeed yields locally structured 2D organic nanosheets. The key is to run the process in the temperature window between crystallization and melting.

Our concept of SPSC is not limited to a special solvent or solvent mixture and can be transferred to other suitable solvents. The prerequisite is that one can control the crystallization and melting of the polymer in solution by temperature. Here, we used ethyl acetate as solvent for the red- and green-labeled vitamin C-PE. First, we need to know the temperature window in which to perform the secondary crystallization process. Since the solubility of the vitamin C polymer in ethyl acetate is very low, there was not enough signal in DSC measurements to determine this window. Instead, we did temperature-dependent

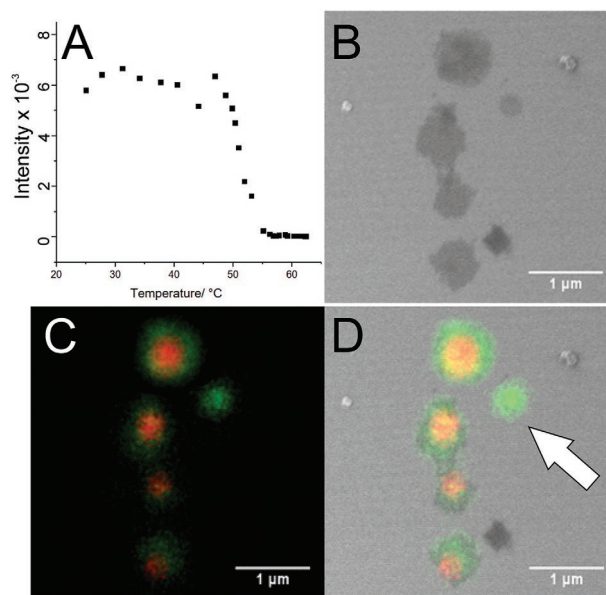


**Figure 4.** Temperature dependent light scattering of a vitamin C-PE nanosheet dispersion in ethyl acetate (A), SEM (B), and cLSM (C) micrographs of SPSC grown single crystal nanosheets from ethyl acetate. The overlay of SEM and cLSM shows the core-rim structure of the laterally structured nanosheets (D).

DLS measurements (**Figure 4a**). Upon heating, the crystals melt at 55 °C. Therefore, we prepared the initial crystals with the red fluorescence label by slowly cooling the solution from  $\approx 70$  °C to room temperature, yielding a dispersion of the initial crystals. Subsequently, this dispersion was carefully heated to 53 °C, just below the melting temperature. Now, a solution of the green-labeled vitamin C-PE was added followed by slow cooling to room temperature. SEM and TEM micrographs reveal the formation of monolayer single 2D crystals (**Figure 4B** and **Figure S6**, Supporting Information). However, electron microscopy cannot display the core-rim structure of the nanosheets due to the lack contrast. Nevertheless, since the SPSC was done with two differently labeled polymers, the cLSM clearly detects the local structure of the core–shell crystalline nanosheets (**Figure 4C**). The overlay of the SEM and the cLSM micrographs in **Figure 4D** finally shows that we obtained locally structured single 2D organic nanosheets. However, in the micrographs in **Figure 4** there is one platelet (arrow in **Figure 4D**), that shows no local structure. It is only composed of the second, green-labeled polymer.

We assume that this platelet was formed due to homogeneous nucleation. However, our SPSC process actually works and allows the formation of nanostructured 2D platelets. Only small adjustments to the process parameters may be necessary to suppress homogeneous nucleation completely.

So far, we have only used a single polymer (vitamin C-PE) for our SPSC process. To further increase the chemical functionality and to achieve a local control on the surface, two chemically different PE-like polymers with different functional groups are used: beside the vitamin C-containing polymer, a polyphosphoester carrying phenyl- and phosphoric acid groups was chosen (**Scheme S2**, Supporting Information). Both polymers

have the same PE sequence length of 20 CH<sub>2</sub> units between the functional groups.

Both polymers, vitamin C and polyphosphoester, were dissolved in ethyl acetate at 70 °C. Subsequently, the polymer solution was cooled down to 20 °C over a period of 25 h. The two polymers have slightly different crystallization temperatures in ethyl acetate. Upon cooling, the polyphosphoester crystallizes first and thus generates the initial seed platelets. Further cooling then induces the crystallization of the vitamin C-PE, which continues the growth of the seeds to form the outer rim of the platelets. As a result, a dispersion of 2D nanosheets with a polyphosphoester core and a vitamin C polymer rim is obtained. It is important to mention that the surface chemistry is different for the core and the shell. Since the phosphate and the vitamin C groups are expelled from the crystal core, these groups are arranged on the surface of the 2D nanosheets. Additionally, due to the chain folding in the crystal, they are arranged with the precision of the crystal lattice.

Even though the obtained 2D nanosheets contain different functional groups, TEM measurement did not reveal any distinct variations in the electron density of the obtained monolayer crystals (Figure S7A, Supporting Information). However, to visualize the local structure, we conducted a site-selective surface functionalization at the alcohol groups of the vitamin C units. We assume to have hydroxyl groups of the vitamin C-polymer at the rim and phosphonate groups from the polyphosphoester polymer at the core. If the platelets are exposed to a trimethylsilyl chloride (TMS-Cl) solution, only the vitamin C units react with the electrophilic TMS-Cl forming a silyl ether bond, while the phosphoesters, on the contrary, do not react. Therefore, we dissolved TMS-Cl in chloroform or in *n*-octane and applied it to the nanostructured polymer platelets, which were already attached to a thin carbon film on a TEM grid. Excess TMS-Cl solution was removed using filter paper, and the 2D nanosheets were inspected by TEM. In the case of addition of TMS-Cl, dissolved in chloroform, a worm-like formation around polymer crystals is observed (Figure 5A). This is very likely due to the good solubility of the vitamin C-polymer in chloroform. The polymer at the rim dissolves and reacts with the TMS-Cl, which explains the system's morphology. However, the polyphosphoester core did not react with the TMS-Cl, so no silyl ether was found in the core region of the platelets.

Using non polar *n*-octane prevents dissolution of initial crystals. In this case, a donut-like structure was observed (Figure 5B). Again, the inner polyphosphoester core does not react with TMS-Cl, while the vitamin C rim was decorated. This observation clearly demonstrates that we can use the SPSC concept for regioselective chemical reactions on 2D nanosheets.

### 3. Conclusion

This study presents a novel concept for creating 2D nanosheets with heterogeneously functionalized surfaces by consecutively crystallizing two precisely synthesized polymers with different functional groups. This concept, which is based on folded polymer crystallization, is highly versatile and straightforward. The functional groups on the surface are accessible and can be used for selective local chemical reactions. Furthermore, these

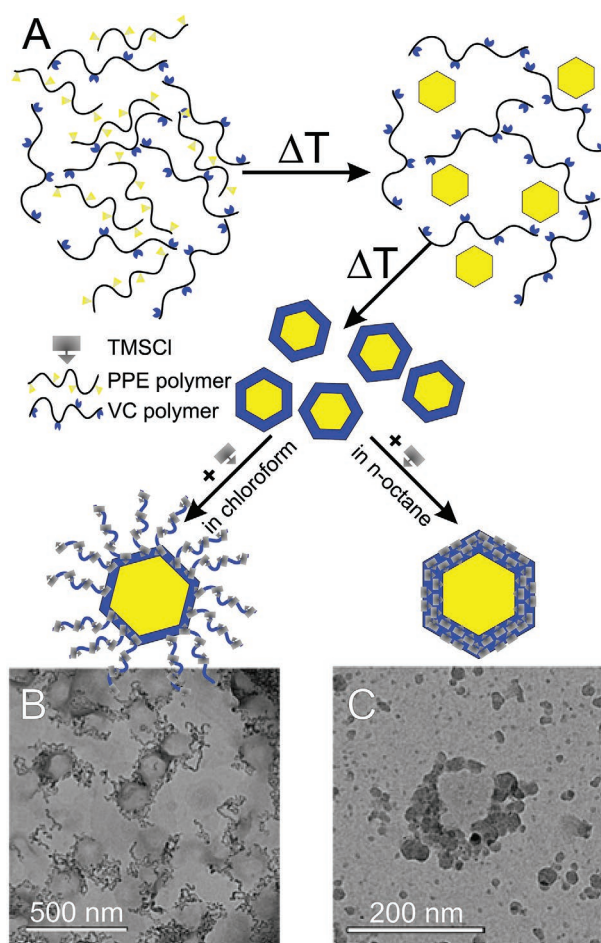


**Figure 5.** Scheme of cocrystallization between vitamin C- polymer and polyphosphoester from hot ethyl acetate and subsequent attachment of chlor(trimethyl)silan molecules to the outer part of the crystals, consisting of VC crystals with functional OH groups (A), TEM bright-field micrograph of obtained solution grown crystal in chloroform (B) and single crystals in *n*-octane (C).

groups are arranged on the surface with the perfection of the crystal lattice. The novelty of our concept is, that it exploits the crystallization of an aliphatic polymer. Here, we used PE, which is the most basic polymer, because it is composed of CH<sub>2</sub> units only. Adjusting the crystallization process via the molecular structure is not necessary. In addition, the choice of the functional group is barely limit and opens up a wide range of possible applications. For example, by inserting thiophene groups, nanosheets with a semiconducting surface can be produced.<sup>[31]</sup> In combination with the local control over the surface chemistry presented here, this concept could find application in molecular electronics. However, the concept presented here is also conceivable in the biomedical field as a drug carrier, for example, if cleavable groups are introduced.

### 4. Experimental Section

Solvents and all commercially available reagents were purchased from Acros Organics and Sigma Aldrich and used as received, unless

otherwise stated. The first generation Grubbs catalyst was purchased from Sigma-Aldrich and stored under argon atmosphere. Deuterated solvents were purchased from Acros Organics and Sigma Aldrich. All solvents were dried using molecular sieves for at least 24 h. Chloroform-d was stored over activated 3 Å molecular sieves and anhydrous sodium carbonate, to quench residual acid.

**Differential Scanning Calorimetry:** Thermal analysis was carried out using a Mettler-Toledo DSC 822. For nonisothermal crystallization, the samples were heated well above the melting point and kept at this temperature for 10 min. Polymer sample was then cooled at the rate of 10 K min<sup>-1</sup> to 0 °C and heated again at the same rate to 120 °C. The second heating was used to determine the melting enthalpy ( $\Delta H_m$ ) and  $T_m$ .

**Transmission Electron Microscopy:** A FEI Tecnai F20 transmission electron microscope operated at an acceleration voltage of 200 kV was used to determine the crystal morphology, thickness, and crystal structure. Bright field (BF) and parallel beam nano-electron diffraction (NBED) were used for measurements. To study the crystallization behavior, polymers were dissolved in THF and crystallized by adding dropwise deionized water while gentle stirring or dissolved in hot ethyl acetate and crystallized slowly during cooling from solution.

**Scanning Electron Microscopy:** Images, providing topographic and material contrasts, were acquired using the LEO Gemini 1530 field-emission scanning electron microscope at (ultra) low (landing) voltages, respectively in the range from 100 to 200 V by using the in-column ring detector Inlens-SE at working distance of  $\approx$ 2 mm and Line Average scan mode. Sample was applied on the ITO substrate from the ethyl acetate solution. Beam damage was considered less relevant/acceptable under the conditions being used.

**Confocal Microscope:** Fluorescence of the crystals was imaged on a Leica TCS SP5 confocal microscope (Leica, Wetzlar) using a HCX PL APO CS 63XNA1.40 oil immersion objective and photomultipliers as detectors. The pinhole was set to 0.5 A.U. in order to increase the resolution. Cy3 fluorophore was excited at 514 nm and emission detected at 539–610 nm. Cy5 was excited at 633 nm and detected at 652–731 nm. Additionally, the sample was excited at 458 nm and reflected light was detected at 452–463 nm to facilitate relocalization of the crystals in SEM.

**Dynamic Light Scattering:** Light scattering measurements were performed on an ALV spectrometer consisting of a goniometer and an ALV-5004 multiple-tau full-digital correlator (320 channels), which allows measurements over an angular range from 30° to 150°. A He-Ne Laser (wavelength of 632.8 nm) was used as light source. For temperature-controlled measurements the light scattering instrument was equipped with a thermostat from Julabo. The sample solution was filtered through low protein binding hydrophilic PTFE membrane filters with a pore size of 0.45  $\mu$ m (LCR Millipore). Measurements were performed at 90° angle at temperatures ranging from 20 to 62 °C using a heating rate of 2.5 °C min<sup>-1</sup>.

**High-Performance Liquid Chromatography:** Covalent bonds between vitamin C-PE and fluorescent dyes Cyanin 3 (Cy3) and Cyanin 5 (Cy5) were confirmed using an Agilent Technologies HPLC with quaternary pump Series 1100, thermostated column compartment Series 1200, diode array detector, ELSD Varian 385-LC. Experiments were conducted using two different columns Macherey-Nagel: Pyramid (RP C18) length: 125 mm / diameter: 3 mm / particle size: 5  $\mu$ m for experiment “c” flow: 0.8 mL min<sup>-1</sup> / 20 °C / gradient of THF–water + 0.1% TFA starting with 40/60; in 5 min 100/0 and HD8 (RP C8-“high-density”) 125/4/5 for experiment “a” flow 1 mL min<sup>-1</sup> / 40 °C / gradient of THF/water + 0.1% TFA starting with 50/50; in 5 min 100/0.

**Synthesis of Vitamin C-PE and Fluorescent Labeling:** Synthesis of PE-like polymer with equidistantly distributed ascorbic acid (vitamin C) groups along the polymer chain and its subsequent labeling with fluorescent dyes Cy3 or Cy5 was conducted according to previously published procedure.<sup>[24]</sup> Synthesis of PE-like polyphosphoester, containing 20% of hydroxyl groups and 80% of phenoxy groups, was prepared according to previously published procedure.<sup>[32]</sup>

**Sample Preparation:** To prepare the samples, we applied either crystallization on a water surface using LBT or crystallization in solution.

Formation of single polymer crystals and crystal growth experiments were conducted in solution to obtain single separate crystals.

**Single Layer Crystals in Ethyl Acetate:** 0.1 mg of vitamin C-PE was dissolved in 1 mL of ethyl acetate. The sample was kept in a temperature-controlled oil bath at 70 °C until full dissolution, then the solution was slowly cooled down to room temperature for crystallization. Afterward, one droplet of the dispersion was dropped onto a carbon-coated grid for TEM measurement.

**In THF–Water Mixture:** Vitamin C-PE was dissolved in THF, after full dissolution deionized water was added dropwise to the sample while stirring. Polymer concentration, solvents ratio, and average size of the lamellar crystals are given in Supporting Information (Figures S2–S5, Supporting Information). After addition of water, the formation of single polymer crystals occurs within a minute. One droplet of the obtained dispersion was applied onto a carbon-coated TEM grid for further measurement.

**Crystal Growth Experiments in Ethyl Acetate:** 0.1 mg of vitamin C-PE was dissolved in 1 mL of ethyl acetate. The sample was kept in a temperature-controlled oil bath at 70 °C until full dissolution, then the solution was slowly cooled down to room temperature for crystallization. To the obtained polymer crystals dispersion, 0.05 or 0.15 mL of PE-VC with concentration 1 mg mL<sup>-1</sup> in THF was added dropwise while stirring. One droplet of the dispersion was applied onto a carbon-coated TEM grid for further measurement.

**In THF–Water Mixture at Room Temperature:** 0.1 mg of vitamin C-PE was dissolved in 600  $\mu$ L of THF, after full dissolution 400  $\mu$ L deionized water was added dropwise to the sample while stirring. To the obtained polymer crystals dispersion 0.05 or 0.15 mL of PE-VC with concentration 1 mg mL<sup>-1</sup> in THF was added dropwise while stirring. One droplet of the dispersion was applied onto a carbon-coated TEM grid for further measurement.

**In THF–Water Mixture at 38 °C:** 0.08 mg of vitamin C-PE was dissolved in 600  $\mu$ L of THF, after full dissolution 400  $\mu$ L deionized water was added dropwise to the sample while stirring. The sample was kept in a temperature-controlled oil bath at 38 °C, 100  $\mu$ L of the vitamin C-PE in THF (0.1 mg mL<sup>-1</sup>) was heated up to 38 °C and added to the mixture during gentle stirring, after 5 min stirring and heating were switched off. After cooling down to the room temperature, one droplet of the polymer crystals dispersion was dropped onto a carbon-coated grid for TEM measurement.

**Polymer Crystals Assembly on LBT:** 0.1 mol% solutions of PE-VC, labeled with fluorescent dyes Cy3 and Cy5, in THF were prepared. For the first experiment, 3–4 drops of each solution were added subsequently on the layer of deionized water on the LBT and leave to evaporate all THF and form polymer crystals. For the second experiment, both solutions were mixed in equal volumes and the obtained mixture was added dropwise on the LBT with deionized water and leave to evaporate all THF and form polymer crystals. Both samples were transferred on the glass slides and measured on the confocal microscope.

**In THF–Water Mixture:** 0.08 mg of labeled vitamin C-PE was dissolved in 600  $\mu$ L of THF, after full dissolution 400  $\mu$ L deionized water was added dropwise to the sample while stirring. The sample was kept in a temperature-controlled oil bath at 38 °C, 100  $\mu$ L of the vitamin C-PE, labeled with the second color, in THF (0.1 mg mL<sup>-1</sup>) was heated up to 38 °C and added to the mixture during gentle stirring, after 5 min stirring and heating were switched off. After cooling down to the room temperature, one droplet of the polymer crystals dispersion was dropped onto a carbon-coated grid for TEM measurement and on the glass slide for the measurement on the confocal microscope.

**In Ethyl Acetate:** 0.08 mg of vitamin C-PE was dissolved in 1 mL of ethyl acetate. The sample was kept in a temperature-controlled oil bath at 70 °C until full dissolution, then the solution was slowly cooled down to room temperature for crystallization. To the obtained crystals dispersion of the polymer, heated up to 53 °C, 0.1 mL of vitamin C-PE, labeled with the second color, with concentration 1 mg mL<sup>-1</sup> in ethyl acetate was heated up to 60 °C and added dropwise while gentle stirring,

in 5 min stirring and heating were switched off. After cooling down to the room temperature, one droplet of the polymer crystals dispersion was dropped onto a carbon-coated grid for TEM measurement and on the glass slide for the measurement on the confocal microscope. The dispersion was stable for at least 1 week.

**Polymer Co-Crystallization:** 0.1 mg of PE-VC and 0.1 mg of polyphosphoester polymers were dissolved in 2 mL ethyl acetate. The mixture was kept in a temperature-controlled oil bath at 70 °C for 1 h while stirring, then stirring was switched off and the sample was cooled down to the room temperature within 25 h. One droplet of the dispersion was dropped onto a carbon-coated grid for TEM measurement.

To functionalize a surface of obtained monolayer crystals, one drop of the sample was applied onto a carbon-coated TEM grid and let it dry. One droplet of trimethylsilyl chloride (TMS-Cl) was dissolved in 1 mL of chloroform (CHCl<sub>3</sub>) or n-octane, added onto the grid with polymer crystals and measured on the TEM.

## Supporting Information

Supporting Information is available from the Wiley Online Library or from the author.

## Acknowledgements

The authors would like to acknowledge the financial support by the Max-Planck Society. The authors thanks go to Beate Müller (MPIP) for HPLC measurements, Christine Rosenauer (MPIP) for DLS measurements, Petra Räder (MPIP) for DSC measurements and Gunnar Glaßer (MPIP) for SEM measurements. The authors thank Dr. Hisaschi Tee (MPIP) for synthetic assistance.

Open access funding enabled and organized by Projekt DEAL.

## Conflict of Interest

The authors declare no conflict of interest.

## Author Contributions

O.S. and I.L. conceived the experiments. O.S. and F.W. developed the synthesis route for the polymers. A.K. planned and performed the SEM and confocal microscopy measurements. K.L., F.W., and I.L. supervised the project.

## Data Availability Statement

The data that support the findings of this study are available from the corresponding author upon reasonable request.

## Keywords

2D organic nanosheets, defect engineering, polymer crystallization, precision polymers, surface functionalization

Received: October 19, 2022

Revised: February 21, 2023

Published online: March 17, 2023

- [1] T. Fujie, *Polym. J.* **2016**, *48*, 773.
- [2] J.-H. Kim, M. Bohra, V. Singh, C. Cassidy, M. Sowwan, *ACS Appl. Mater. Interfaces* **2014**, *6*, 13339.
- [3] T. Fujie, J. Y. Park, A. Murata, N. C. Estillore, M. C. R. Tria, S. Takeoka, R. C. Advincula, *ACS Appl. Mater. Interfaces* **2009**, *1*, 1404.
- [4] I. Insua, J. Bergueiro, A. Méndez-Ardoy, I. Lostalé-Seijo, J. Montenegro, *Chem. Sci.* **2022**, *13*, 3057.
- [5] T. Kim, J. Y. Park, J. Hwang, G. Seo, Y. Kim, *Adv. Mater.* **2020**, *32*, 2002405.
- [6] S. Yang, S.-Y. Kang, T.-L. Choi, *Nat. Commun.* **2021**, *12*, 2602.
- [7] F. Jiao, Y. Chen, H. Jin, P. He, C.-L. Chen, J. J. De Yoreo, *Adv. Funct. Mater.* **2016**, *26*, 8960.
- [8] Y. Song, M. Wang, S. Akkineni, W. Yang, J. J. Hettige, H. Jin, Z. Liao, P. Mu, F. Yan, M. Baer, J. J. De Yoreo, D. Du, Y. Lin, C.-L. Chen, *ACS Mater. Lett.* **2021**, *3*, 420.
- [9] H. Jin, F. Jiao, M. D. Daily, Y. Chen, F. Yan, Y.-H. Ding, X. Zhang, E. J. Robertson, M. D. Baer, C.-L. Chen, *Nat. Commun.* **2016**, *7*, 12252.
- [10] Y. Lin, M. R. Thomas, A. Gelmi, V. Leonardo, E. T. Pashuck, S. A. Maynard, Y. Wang, M. M. Stevens, *J. Am. Chem. Soc.* **2017**, *139*, 13592.
- [11] A. D. Merg, E. Van Genderen, A. Bazrafshan, H. Su, X. Zuo, G. Touponse, T. B. Blum, K. Salaita, J. P. Abrahams, V. P. Conticello, *J. Am. Chem. Soc.* **2019**, *141*, 20107.
- [12] T. Sakurai, N. Orito, S. Nagano, K. Kato, M. Takata, S. Seki, *Mater. Chem. Front.* **2018**, *2*, 718.
- [13] Y. Li, J. Li, S. Du, Z. Wang, B.-L. Gu, S.-C. Zhang, K. He, W. Duan, Y. Xu, *Sci. Adv.* **2019**, *5*, aaw9120.
- [14] S. Agbolaghi, M. Alizadeh-Osgouei, S. Zenoozi, S. Abbaspoor, F. Abbasi, *J. Nanostructure. Chem.* **2016**, *7*, 15.
- [15] N. Hasan, C. Schwieger, H. T. Tee, F. R. Wurm, K. Busse, J. Kressler, *Eur. Polym. J.* **2018**, *101*, 350.
- [16] P. Ortmann, J. Trzaskowski, M. Krumova, S. Mecking, *ACS Macro Lett* **2013**, *2*, 125.
- [17] Z. M. Hudson, C. E. Boott, M. E. Robinson, P. A. Rugar, M. A. Winnik, I. Manners, *Nat. Chem.* **2014**, *6*, 893.
- [18] Z. M. Hudson, D. J. Lunn, M. A. Winnik, I. Manners, *Nat. Commun.* **2014**, *5*, 3372.
- [19] A. Keller, *Philos. Mag.* **1957**, *2*, 1171.
- [20] E. W. Fischer, *Z. Naturforsch., A: Phys. Sci.* **1957**, *12*, 753.
- [21] T. Haider, O. Suraeva, M. L. O'duill, J. Mars, M. Mezger, I. Lieberwirth, F. R. Wurm, *Polym. Chem.* **2020**, *11*, 3404.
- [22] M. D. Schulz, K. B. Wagener, *Macromol. Chem. Phys.* **2014**, *215*, 1936.
- [23] J. C. Markwart, O. Suraeva, T. Haider, I. Lieberwirth, R. Graf, F. R. Wurm, *Polym. Chem.* **2020**, *11*, 7235.
- [24] O. Suraeva, C. Champanhac, V. Mailänder, F. R. Wurm, H. Weiss, R. Berger, M. Mezger, K. Landfester, I. Lieberwirth, *Macromolecules* **2020**, *53*, 2932.
- [25] S. Luleburgaz, M. Abuaf, U. Tunca, G. Hizal, H. Durmaz, *Macromol. Rapid Commun.* **2017**, *38*, 1600772.
- [26] L. Zhao, P. Choi, *Mater. Manuf. Processes* **2006**, *21*, 135.
- [27] B. Crist, M. J. Hill, *J. Polym. Sci., Part B: Polym. Phys.* **1997**, *35*, 2329.
- [28] D. J. Blundell, A. Keller, *J. Macromol. Sci., Part B Phys.* **2006**, *2*, 301.
- [29] H. M. L. Lambermont-Thijs, H. P. C. V. Kuringen, J. P. W. V. D. Put, U. S. Schubert, R. Hoogenboom, *Polymers* **2010**, *2*, 188.
- [30] L. Xu, H. Zhang, Y. Lu, L. An, T. Shi, *Polymer* **2020**, *190*, 122259.
- [31] O. Suraeva, B. Jeong, K. Asadi, K. Landfester, F. R. Wurm, I. Lieberwirth, *Polym. Chem.* **2021**, *12*, 2045.
- [32] Y.-R. Zheng, H. T. Tee, Y. Wei, X.-L. Wu, M. Mezger, S. Yan, K. Landfester, K. Wagener, F. R. Wurm, I. Lieberwirth, *Macromolecules* **2016**, *49*, 1321.